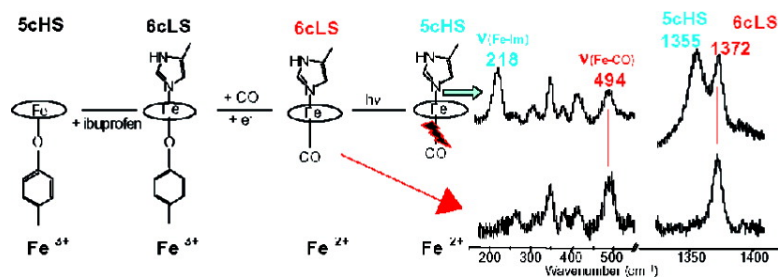


Ibuprofen Induces an Allosteric Conformational Transition in the Heme Complex of Human Serum Albumin with Significant Effects on Heme Ligation

Francesco P. Nicoletti, Barry D. Howes, Maria Fittipaldi, Gabriella Fanali, Mauro Fasano, Paolo Ascenzi, and Giulietta Smulevich

J. Am. Chem. Soc., **2008**, 130 (35), 11677-11688 • DOI: 10.1021/ja800966t • Publication Date (Web): 06 August 2008

Downloaded from <http://pubs.acs.org> on February 8, 2009



More About This Article

Additional resources and features associated with this article are available within the HTML version:

- Supporting Information
- Access to high resolution figures
- Links to articles and content related to this article
- Copyright permission to reproduce figures and/or text from this article

[View the Full Text HTML](#)

Ibuprofen Induces an Allosteric Conformational Transition in the Heme Complex of Human Serum Albumin with Significant Effects on Heme Ligation

Francesco P. Nicoletti,[†] Barry D. Howes,[†] Maria Fittipaldi,^{†,‡} Gabriella Fanali,[§] Mauro Fasano,[§] Paolo Ascenzi,^{||,⊥} and Giulietta Smulevich^{*,†}

Dipartimento di Chimica and INSTM, Università di Firenze, Via della Lastruccia 3, I-50019 Sesto Fiorentino (FI), Italy, Dipartimento di Biologia Strutturale e Funzionale, and Centro di Neuroscienze, Università dell'Insubria, Via Alberto da Giussano 12, I-21052 Busto Arsizio (VA), Italy, Centro Interdipartimentale di Microscopia Elettronica, Università Roma Tre, Via della Vasca Navale 79, I-00146 Roma, Italy, and Istituto Nazionale per le Malattie Infettive I.R.C.C.S. 'Lazzaro Spallanzani', Via Portuense 292, I-00149 Roma, Italy

Received February 7, 2008; Revised Manuscript Received May 27, 2008; E-mail: giulietta.smulevich@unifi.it

Abstract: Human serum albumin (HSA), the most prominent protein in blood plasma, is able to bind a wide range of endogenous and exogenous compounds. Among the endogenous ligands, HSA is a significant transporter of heme, the heme–HSA complex being present in blood plasma. Drug binding to heme–HSA affects allosterically the heme affinity for HSA and vice versa. Heme–HSA, heme, and their complexes with ibuprofen have been characterized by electronic absorption, resonance Raman, and electron paramagnetic resonance (EPR) spectroscopy. Comparison of the results for the heme and heme–HSA systems has provided insight into the structural consequences on the heme pocket of ibuprofen binding. The pentacoordinate tyrosine-bound heme coordination of heme–HSA, observed in the absence of ibuprofen, becomes hexacoordinate low spin upon ibuprofen binding, and heme dissociates at increasing drug levels. The electronic absorption spectrum and $\nu(\text{Fe–CO})/\nu(\text{CO})$ vibrational frequencies of the CO–heme–HSA–ibuprofen complex, together with the observation of a Fe–His Raman mode at 218 cm^{-1} upon photolysis of the CO complex and the low spin EPR g values indicate that a His residue is one of the low spin axial ligands, the sixth ligand probably being Tyr161. The only His residue in the vicinity of the heme Fe atom is His146, 9 \AA distant in the absence of the drug. This indicates that drug binding to heme–HSA results in a significant rearrangement of the heme pocket, implying that the conformational adaptability of HSA involves more than the immediate vicinity of the drug binding site. As a whole, the present spectroscopic investigation supports the notion that HSA could be considered as the prototype of monomeric allosteric proteins.

Introduction

Human serum albumin (HSA), the most prominent protein in plasma, has the capability to bind a wide range of endogenous and exogenous compounds such as nonesterified fatty acids, heme, bilirubin, thyroxine, and bile acids, as well as a huge variety of drugs.^{1–5} Its extraordinary ligand binding capacity

derives from the adaptability of the HSA structure to very diverse ligands and from the presence of a variety of binding sites. In fact, HSA consists of a α -helical monomer of 66 kDa containing three homologous domains (I–III), each of which is composed by two subdomains, named A and B, connected by random coils. Terminal regions of sequential domains contribute to the formation of interdomain regions linking domain IB to IIA and IIB to IIIA (Figure 1, panel A).^{6–10} According to Sudlow's nomenclature, two primary sites (1 and 2) have been identified for ligand binding to HSA. Warfarin, an anticoagulant drug, and ibuprofen, a nonsteroidal anti-inflammatory agent, have been considered as stereotypical ligands for Sudlow's site 1 and 2, respectively.¹¹ Warfarin, as

[†] Dipartimento di Chimica, Università di Firenze.

[‡] INSTM, Università di Firenze.

[§] Università dell'Insubria.

^{||} Università Roma Tre.

[⊥] Istituto Nazionale per le Malattie Infettive I.R.C.C.S. 'Lazzaro Spallanzani'.

- (1) Fasano, M.; Curry, S.; Terreno, E.; Galliano, M.; Fanali, G.; Narciso, P.; Notari, S.; Ascenzi, P. *IUBMB Life* **2005**, *57*, 787–796.
- (2) Ascenzi, P.; Bocedi, A.; Notari, S.; Fanali, G.; Fesce, R.; Fasano, M. *Mini Rev. Med. Chem.* **2006**, *6*, 483–489.
- (3) Ghuman, J.; Zunszain, P. A.; Petitpas, I.; Bhattacharya, A. A.; Ottagiri, M.; Curry, S. *J. Mol. Biol.* **2005**, *353*, 38–52.
- (4) Simard, J. R.; Zunszain, P. A.; Ha, C. E.; Yang, J. S.; Bhagavan, N. V.; Petitpas, I.; Curry, S.; Hamilton, J. A. *Proc. Natl. Acad. Sci. U.S.A.* **2005**, *102*, 17958–17963.
- (5) Simard, J. R.; Zunszain, P. A.; Hamilton, J. A.; Curry, S. *J. Mol. Biol.* **2006**, *361*, 336–351.

(6) He, X.; Carter, D. C. *Nature* **1992**, *358*, 209–215.

(7) Carter, D. C.; Ho, J. X. *Adv. Protein Chem.* **1994**, *45*, 153–203.

(8) Peters, T., Jr. *All about Albumin: Biochemistry, Genetics and Medical Applications*; Academic Press: Orlando, FL, 1996.

(9) Sugio, S.; Kashima, A.; Mochizuki, S.; Noda, M.; Kobayashi, K. *Protein Eng.* **1999**, *12*, 439–446.

(10) Curry, S. *Vox Sang.* **2002**, *83* (Suppl. 1), 315–319.

(11) Sudlow, G.; Birkett, D. J.; Wade, D. N. *Mol. Pharmacol.* **1975**, *11*, 824–832.

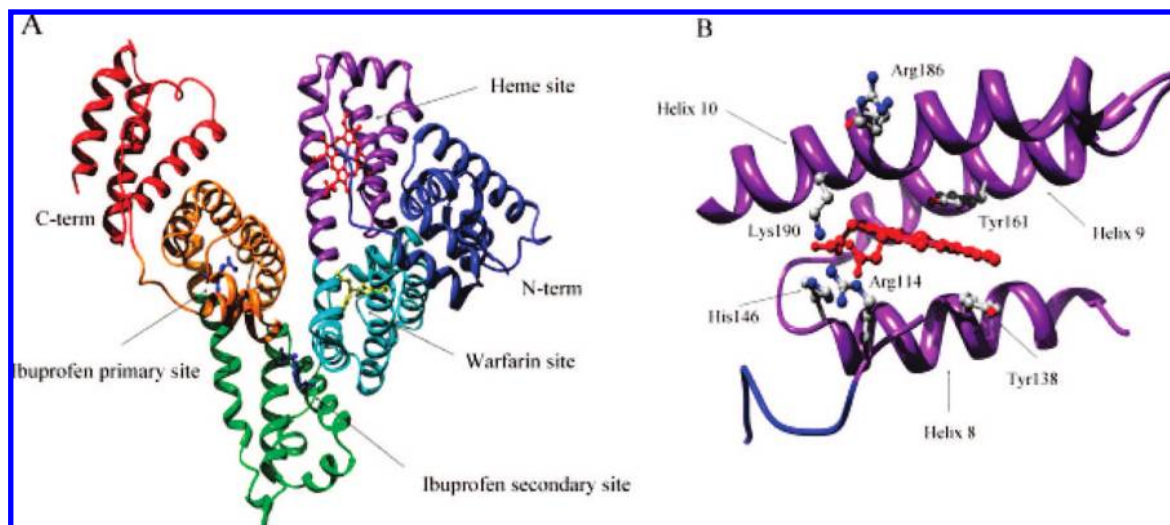


Figure 1. Panel A: HSA structure. The six subdomains of HSA are colored as follows: subdomain IA, blue; subdomain IB, purple; subdomain IIA, cyan; subdomain IIB, green; subdomain IIIA, orange; subdomain IIIB, red. The heme (red) binds in the primary cleft of subdomain IB. Ibuprofen (blue) is shown in both its primary (Sudlow's site 2) and secondary binding sites. Warfarin (yellow) occupies its primary binding site (Sudlow's site 1). N- and C-termini are labeled. Atomic coordinates are taken from PDB entries 1N5U,¹³ 1O9X,¹⁴ 2BXD,³ and 2BXG.^{3,14} Panel B: Zoom of the heme binding pocket. Heme (red) is bound in the cleft formed by helices 8, 9, and 10. Residues Arg114, Tyr138, His 146, Tyr161 (coordinating heme Fe^{3+}), Arg186, and Lys190 are shown.

other bulky heterocyclic anions, binds to Sudlow's site 1 located in subdomain IIA, whereas ibuprofen, as other aromatic carboxylates with an extended conformation, prefers Sudlow's site 2, located in subdomain IIIA (Figure 1, panel A).³ In addition, a secondary binding cleft has been found for ibuprofen located at the interface between subdomains IIA and IIB.^{3,7,10,11}

Among the various endogenous ligands, HSA transiently binds heme, participating in its transfer to the liver. Although under physiological conditions plasma heme is mainly bound to hemopexin, which delivers it to the liver via a receptor-mediated uptake mechanism,⁸ HSA acts as a depot for heme overflow when hemopexin becomes saturated (i.e., following intravascular acute hemolysis).^{8,12} Heme is then gradually transferred from HSA to hemopexin, that allows the receptor-mediated reuptake by parenchymal liver cells. The primary heme binding site is located within domain I of HSA (Figure 1).^{13–15} However, the heme affinity for HSA depends on the presence of other ligands bound to HSA. Indeed, its dissociation equilibrium constant (i.e., K_d) increases from 1.1×10^{-8} M in the absence of drugs to 1.5×10^{-7} M in the presence of Sudlow's site 1 ligands, the heme and the warfarin (Sudlow site 1) binding sites being spectroscopically and functionally coupled.^{16,17} As a consequence, while HSA abundance makes it an important factor in the pharmacokinetic and in the pharmacodynamic behavior of many drugs, including their efficacy and rate of delivery, the existence of (anti)cooperativity and allosteric modulation within different binding sites result in competition between exogenous and endogenous ligands.

Therefore, it is of interest to investigate the structural basis of coupling between different binding sites.

In the present study, the characterization of the unusual axial coordination in both the ferric and ferrous forms of the heme Fe atom of the naturally occurring heme–HSA complex by UV–vis, resonance Raman (RR) and electron paramagnetic resonance (EPR) spectroscopies is reported. In the absence of an X-ray structure of the ternary heme–HSA–ibuprofen complex, an important aspect of this study was to gain insight into the structural changes of the HSA heme binding site induced allosterically by drug binding. Ibuprofen binding to heme–HSA is found to induce significant structural variations of the heme cavity.

Materials and Methods

Materials. Fatty-acid free HSA, hemin chloride, and ibuprofen were obtained from Sigma-Aldrich. Gaseous CO and ^{13}CO were purchased from Rivoira and FluoroChem, respectively. Sodium dithionite was obtained from Fluka Chemicals. All the other chemicals were obtained from Merck AG. All chemicals were of analytical or reagent grade and were used without further purification.

Sample Preparation. Heme (hemin or Fe(III) protoporphyrin IX, Fe–PPIX) was dissolved in 0.1 M NaOH to give a final concentration of 2–3 mM. An appropriate amount of this solution was added to HSA in phosphate-buffered saline (PBS) to give a final heme–HSA ratio of 1:4. A heme:HSA ratio of 1:4 was employed, rather than the 1:1 ratio used in previous reports,^{18,19} since titration of heme with HSA revealed progressive variations in the heme absorption spectrum reaching a final form for the 1:4 molar ratio (data not shown). Ferric heme–HSA and ferrous heme samples were prepared by addition of 5% volume freshly prepared sodium dithionite (20 mg/mL) to deoxygenated ferric solutions. The ferrous heme–HSA and heme complexes with 2-methylimidazole (2-MeIm) were prepared with a heme:2-MeIm molar ratio of 1:15000 and 1:33000, respectively, using a fresh solution of 2-MeIm in PBS. A higher concentration of 2-MeIm caused the loss of the

- (12) Pasternack, R. F.; Gibbs, E. J.; Hoeflin, E.; Kosar, W. P.; Kubera, G.; Skowronek, C. A.; Wong, N. M.; Muller-Eberhard, U. *Biochemistry* **1983**, *22*, 1753–1758.
- (13) Wardell, M. Z.; Wang, J. X.; Ho, J.; Robert, J.; Rüker, F.; Ruble, J.; Carter, D. C. *Biochem. Biophys. Res. Commun.* **2002**, *291*, 813–819.
- (14) Zunszain, P. A.; Ghuman, J.; Komatsu, T.; Tsuchida, E.; Curry, S. *BMC Struct. Biol.* **2003**, *3*, 6.
- (15) Adams, P. A.; Berman, M. C. *Biochem. J.* **1980**, *191*, 95–102.
- (16) Baroni, S.; Mattu, M.; Vannini, A.; Cipollone, R.; Aime, S.; Ascenzi, P.; Fasano, M. *Eur. J. Biochem.* **2001**, *268*, 6214–6220.
- (17) Ascenzi, P.; Bocedi, A.; Notari, S.; Menegatti, E.; Fasano, M. *Biochem. Biophys. Res. Commun.* **2005**, *334*, 481–486.

- (18) Kamal, J. K. A.; Behere, D. V. *J. Biol. Inorg. Chem.* **2002**, *7*, 273–283.
- (19) Komatsu, T.; Ohmichi, N.; Nakagawa, A.; Zunszain, P. A.; Curry, S.; Tsuchida, E. *J. Am. Chem. Soc.* **2005**, *127*, 15933–15942.

heme from the HSA binding site. It is noted that 2-MeIm does not bind to ferric heme-HSA since no spectral changes have been observed upon addition of this exogenous ligand. The complexes with ibuprofen were prepared by adding a fresh solution of ibuprofen in PBS to the ferric heme-HSA or heme solutions to obtain the molar ratios reported in the text.

All CO-heme complexes were prepared by degassing the free heme or heme-HSA solution by flushing first with nitrogen and then with CO or ^{13}C O and reducing the heme by addition of a 5% volume freshly prepared sodium dithionite (20 mg/mL) solution.

The low temperature measurements were recorded in bicine (*N,N*-bis(2-hydroxyethyl)glycine) buffer for the samples without ibuprofen and in PBS for those in the presence of the drug, since bicine was found to interact with ibuprofen. The room temperature electronic absorption and RR spectra were identical for the samples without ibuprofen prepared in PBS and bicine buffers. The heme concentration of the heme-HSA samples was determined using the molar absorptivity of $99.2 \text{ mM}^{-1} \text{ cm}^{-1}$ at 404 nm.¹⁸ A heme concentration of 9–90 μM was used for room temperature electronic absorption and RR spectra. The heme concentration of the heme-HSA sample for low temperature electronic absorption was 24 μM . The heme concentration for EPR spectroscopy was 60 and 120 μM for samples with and without ibuprofen, respectively.

Spectroscopy. Electronic absorption spectra were measured with a double-beam Cary 5 spectrophotometer (Varian, Palo Alto, CA). The room temperature electronic absorption spectra were obtained using a 5-mm NMR tube or a 1-mm cuvette, and a 600 nm/min scan rate. The RR spectra were obtained using a 5-mm NMR tube and by excitation with the 406.7 and 413.1 nm lines of a Kr+ laser (Coherent, Innova 300 C, Santa Clara, CA), the 488, 496.5, 501.7, and 514.5 nm lines of an Ar+ laser (Coherent, Innova 90/5, Santa Clara, CA), and 441.6 nm line of a HeCd laser (Kimmon IK4121R-G, Tokyo Japan). Backscattered light from a slowly rotating NMR tube was collected and focused into a triple spectrometer (consisting of two Acton Research SpectraPro 2300i and a SpectraPro 2500i in the final stage with a 1800 or 3600 grooves/mm grating) working in the subtractive mode, equipped with a liquid nitrogen-cooled CCD detector. It should be noted that the spectral resolution of the RR spectra cited in the figure captions is that calculated theoretically on the basis of the optical properties of the spectrometer. However, for the moderately broad experimental RR bands observed in the present study (ca. 10 cm^{-1}), the effective spectral resolution will in general be lower.

The low-temperature experiments were carried out using an Air Products Displex closed-cycle He refrigerator with automatic temperature control. The absorption spectra were obtained using a 3-mm quartz microcuvette (100 μL) and a 120 nm/min scan rate. The cuvette was mounted on the coldfinger of the cryostat and filled with the protein solution at 90 K under nitrogen flow. The temperature was then lowered to 11 K under vacuum. The temperature was allowed to stabilize for 30 min before recording the spectrum.

All RR measurements were repeated several times under the same conditions to ensure reproducibility. To improve the signal/noise ratio, a number of spectra were accumulated and summed only if no spectral differences were noted. The RR spectra were calibrated with indene, CCl_4 , dimethyl sulfoxide, acetone, and acetonitrile as standards to an accuracy of $\pm 1 \text{ cm}^{-1}$ for intense isolated bands. To determine peak intensities and positions a curve-fitting program (Lab Calc, Galactic) was used to simulate the spectra using a Lorentzian line shape. A Lorentzian line width of 10 and 12 cm^{-1} was used for the ν_{10} and vinyl modes, respectively.

EPR spectra were recorded on a Bruker Elexys E500 instrument, equipped with an NMR gaussmeter and a microwave frequency counter. An Oxford Instruments ESR 900 cryostat was used to obtain low temperatures. The spectra were recorded under nonsaturating conditions at 5 K, 1 mW microwave power, and 1 mT modulation amplitude. The EPR simulation program used to

determine the g values (Xsophe, Bruker) is appropriate for effective $S = 1/2$ systems.²⁰

Structure Analysis. Coordinates of HSA complexes with heme (PDB entries 1N5U¹³ and 1O9X¹⁴), ibuprofen (PDB entry 2BXG³), and warfarin (PDB entry 2BXD³) were analyzed using UCSF Chimera.²¹ Ray-traced images were produced with Pov-Ray (Persistence of Vision Pty. Ltd., Williamstown, Victoria, Australia. <http://www.povray.org/>).

Results

(Fe³⁺)Heme-HSA. Crystallographic studies¹³ have revealed that the heme bound to its primary site in HSA is buried in a hydrophobic pocket within domain I delimited by Tyr138 and Tyr161 that interact with the porphyrin by π - π stacking. The heme propionates protrude from the pocket pointing toward the interface between domains I and III and are stabilized by salt bridges with His146 and Lys190 (Figure 1, panel B). The structure suggests a weak coordination between the heme Fe atom and the phenolic oxygen of Tyr161 (Fe-O_{Tyr161} distance = 2.73 Å).

The UV-vis electronic absorption spectrum of the ferric heme-HSA (molar ratio 1:4) complex in PBS (0.08 M) at pH 6.9 (Figure 2, panel A, trace a) is characterized by a Soret band at 404 nm, Q₁ and Q₀ bands at 501 and 533 nm, respectively, and the charge-transfer (CT1) band (long wavelength (> 600 nm) porphyrin-to-metal charge transfer band) at 622 nm. The spectrum is almost identical to those previously reported for the heme-HSA complex with a molar ratio 1:1.^{18,19} Moreover, as previously noted,¹⁹ the spectrum is also similar to those of pentacoordinate (5c) high spin (HS) heme proteins with a weakly coordinated tyrosinate ligand.^{19,22–26} Accordingly, the corresponding RR spectra (Figure 2, panel C; Table 1), obtained with excitation wavelengths in resonance with the Soret and Q₁ bands, are characteristic of a 5cHS species (ν_3 at 1493 cm^{-1} , ν_2 at 1568 cm^{-1} , ν_{10} at 1624 cm^{-1}). In addition, the small intensity ratio, $I_{\nu_4}/I_{\nu_3} = 1.4$, observed in the RR spectrum obtained with Soret excitation (Figure 2, panel C, trace a) confirms the presence of a weak bond between an axial oxygen anionic ligand and the Fe atom.^{25,27,28} In tyrosinate-ligated hemoproteins, excitation in the tyrosinate-Fe(III) CT band (near 500 nm) yields characteristic vibrational frequencies for bound phenolate. The most prominent of these bands are $\nu(\text{C}=\text{C})_{\text{ring}}$ at ca. 1600 and ca. 1500 cm^{-1} , $\nu(\text{C}-\text{O})$ at ca. 1300 cm^{-1} and $\nu(\text{Fe}-\text{O})$ at ca. 590 cm^{-1} .^{23,26,29–32} However, the weakness of the

- (20) Hanson, G. R.; Gates, K. E.; Noble, C. J.; Griffin, M.; Mitchell, A.; Benson, S. *J. Inorg. Biochem.* **2004**, *98*, 903–916.
- (21) Pettersen, E. F.; Goddard, T. D.; Huang, C. C.; Couch, G. S.; Greenblatt, D. M.; Meng, E. C.; Ferrin, T. E. *J. Comput. Chem.* **2004**, *25*, 1605–1612.
- (22) Adachi, S.; Nagano, S.; Watanabe, Y.; Ishimori, K.; Morishima, I. *Biochim. Biophys. Res. Commun.* **1991**, *180*, 138–144.
- (23) Adachi, S.; Nagano, S.; Ishimori, K.; Watanabe, Y.; Morishima, I.; Egawa, T.; Kitagawa, T.; Makino, R. *Biochemistry* **1993**, *32*, 241–252.
- (24) Hildebrand, D. P.; Burk, D. L.; Maurus, R.; Ferrer, J. C.; Brayer, G. D.; Mauk, A. G. *Biochemistry* **1995**, *34*, 1997–2005.
- (25) Eakanunkul, S.; Lukat-Rodgers, G. S.; Sumithran, S.; Ghosh, A.; Rodgers, K. R.; Dawson, J. H.; Wilks, A. *Biochemistry* **2005**, *44*, 13179–13191.
- (26) Pond, A. E.; Roach, M. P.; Sono, M.; Rux, A. H.; Franzen, S.; Hu, R.; Thomas, M. R.; Wilks, A.; Dou, Y.; Ikeda-Saito, M.; Ortiz de Montellano, P. R.; Woodruff, W. H.; Boxer, S. G.; Dawson, J. H. *Biochemistry* **1999**, *38*, 7601–7608.
- (27) Hu, S.; Kincaid, J. R. *FEBS Lett.* **1992**, *314*, 293–296.
- (28) Lukat-Rodgers, G. S.; Rodgers, K. R.; Caillet-Saguy, C.; Izadi-Pruneyre, N.; Lecroisey, A. *Biochemistry* **2008**, *47*, 2087–2098.
- (29) Nagai, M.; Yoneyama, Y.; Kitagawa, T. *Biochemistry* **1989**, *28*, 2418–2422.

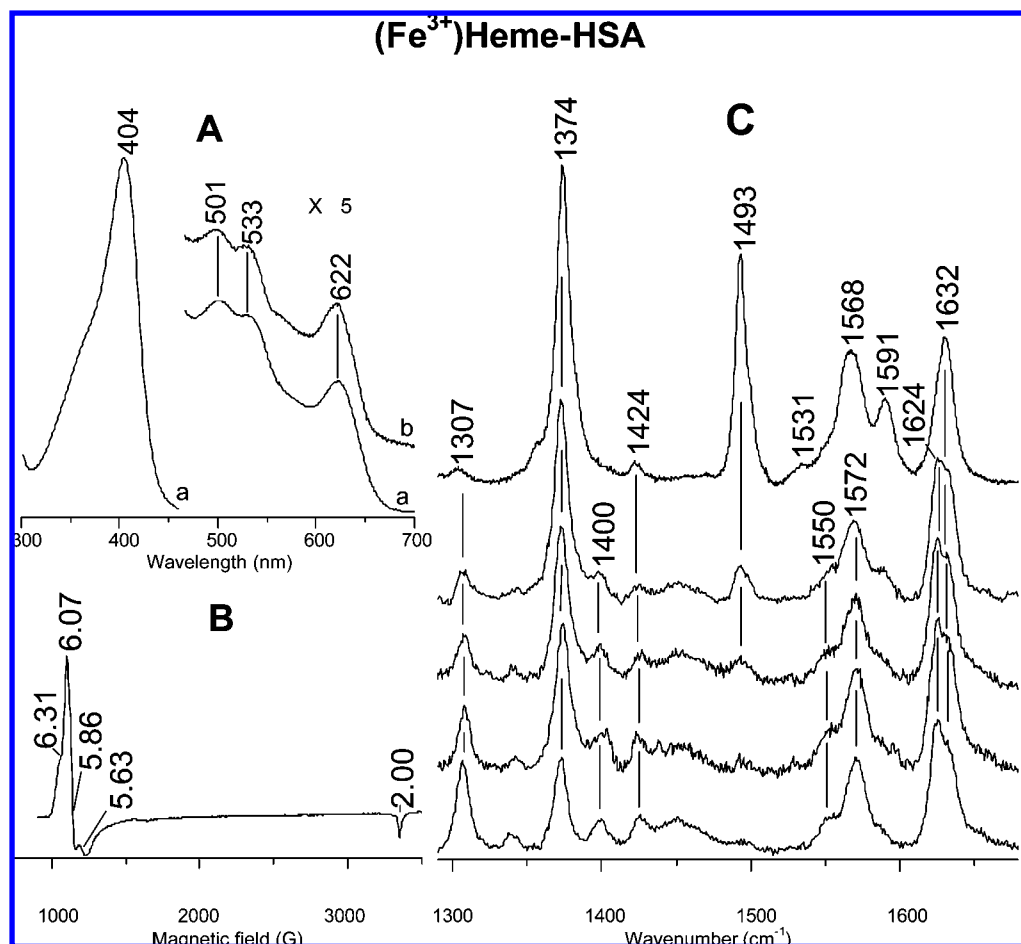


Figure 2. Panel A: absorption spectra of (Fe³⁺)heme–HSA at pH 6.9 in 0.08 M PBS at 298 K (a) and in 0.1 M bicine at 11 K (b). Panel B: X-band EPR spectrum of (Fe³⁺)heme–HSA in 0.1 M bicine at pH 6.9. The spectrum was recorded at 5 K, 1 mW microwave power, and 10 G modulation amplitude. Panel C: RR spectra of (Fe³⁺)heme–HSA in 0.08 M PBS at pH 6.9. Experimental conditions: (a) 406.7 nm excitation wavelength, 15 mW laser power at the sample, 1 cm⁻¹ spectral resolution, average of two spectra with 900 s integration time; (b) 488 nm excitation wavelength, 75 mW laser power at the sample, 2.4 cm⁻¹ spectral resolution, average of four spectra with 480 s integration time; (c) 496.5 nm excitation wavelength, 80 mW laser power at the sample, 2.4 cm⁻¹ spectral resolution, 480 s integration time; (d) 501.7 nm excitation wavelength, 36 mW laser power at the sample, 2.3 cm⁻¹ spectral resolution, average of two spectra with 1000 s integration time; (e) 514.5 nm excitation wavelength, 75 mW laser power at the sample, 2.2 cm⁻¹ spectral resolution, average of four spectra with 960 s integration time. The intensities are normalized to that of the 1632 cm⁻¹ band.

Table 1. Resonance Raman Frequencies (cm⁻¹) of the Heme States Observed for Heme–HSA and Its Complexes with Ibuprofen and 2-Melm

mode	heme–HSA			heme–HSA–ibuprofen		heme–HSA–2Melm	
	Fe ³⁺	Fe ²⁺		Fe ³⁺		Fe ²⁺	
	5cHS	4cIS	5cHS	5cHS	6cLS	5cHS	6cLS
ν_4	1374	1370	1358	1373	1373	1358	1358
ν_3	1493	1502	1472	1493	1502	1472	1493
ν_{11}	1550			1553	1564	1555	
ν_2	1568	1580	1557	1570	1580	1562	1582
ν_{19}	1572						
ν_{37}	1591			1586			
ν_{10}	1624	1635	1602	1626	1639	1607	1623
$\nu_{(C=C)}$	1632	1629	1629	1630	1630	1629	1629

Fe³⁺–O_{Tyr161} bond precluded any enhancement of the Tyr–Fe modes in the RR spectra of the heme–HSA complex for excitation in the Q-band region [Figure 2, panel C, traces b–e], as reported previously for another Tyr–Fe protein, the cyto-

chrome c maturation protein (CcmE).³³ On the basis of depolarization ratio measurements, the RR band observed at 1632 cm⁻¹ for all excitation wavelengths is assigned to the stretching modes of the two vinyl groups, and the band which gains intensity at 1624 cm⁻¹ for excitation in the Q₁ band region (Figure 2, panel C, traces b–e) is assigned to the 5cHS ν_{10} mode. A discussion of these assignments and the properties of the vinyl groups is given in Supporting Information (Figure S1).

Since the electronic absorption spectrum of (Fe³⁺)heme–HSA does not change at low temperature (down to 11 K) (Figure 2, panel A, trace b), low-temperature (5 K) X-band EPR spectroscopy was carried out to obtain further details on the spin state and heme coordination environment of heme–HSA (Figure 2, panel B). In accord with the observation of a HS state in the UV–vis and RR spectra, two HS heme species were identified with $g = 6.07, 5.86, 2.00$ and $g = 6.31, 5.63, 2.00$. The low rhombicity of the EPR signals, $R = 1\%$ and 4% , (the percentage rhombicity is defined as $R = (\Delta g/16) \times 100$, where

(30) Egeberg, K. D.; Springer, B. A.; Martinis, S. A.; Sliagar, S. G.; Morikis, D.; Champion, P. M. *Biochemistry* **1990**, *29*, 9783–9791.

(31) Nagai, K.; Kagimoto, T.; Hayashi, A.; Taketa, F.; Kitagawa, T. *Biochemistry* **1983**, *22*, 1305–1311.

(32) Liu, Y.; Moenne-Loccoz, P.; Hildebrand, D. P.; Wilks, A.; Loehr, T. M.; Mauk, A. G.; Ortiz de Montellano, P. R. *Biochemistry* **1999**, *38*, 3733–3743.

(33) Uchida, T.; Stevens, J. M.; Daltrop, O.; Harvat, E. M.; Hong, L.; Ferguson, S. J.; Kitagawa, T. *J. Biol. Chem.* **2004**, *279*, 51981–51988.

Δg is the absolute difference in g values between the two components near $g = 6$)³⁴ is similar to that of other 5cHS proteins with tyrosine as the axial ligand.^{25,35,36} The structural effects which determine the presence of two HS forms are unclear but likely reflect some flexibility in the geometric disposition of the weakly bound Tyr161 residue and its hydrogen bonding interaction with the nearby water molecule.¹³ If this is the case, it is reasonable to propose that the species displaying lower rhombicity ($g = 6.07, 5.86, 2.00$) is distinguished by a relatively weaker H-bonding interaction.

To summarize, the spectroscopic characterization of $(\text{Fe}^{3+})\text{heme-HSA}$ is consistent with a 5cHS heme and a weak $\text{Fe}^{3+}-\text{O}_{\text{Tyr}}$ coordination, in agreement with the fairly long $\text{Fe}^{3+}-\text{O}$ distance (2.73 Å) determined from the crystal structure.

$(\text{Fe}^{2+})\text{Heme-HSA}$. Further evidence of the weakness of the $\text{Fe}-\text{O}$ bond was obtained by the characterization of the $(\text{Fe}^{2+})\text{heme-HSA}$ and its complex with 2-methylimidazole (2-MeIm). In agreement with previous results,^{18,19} the UV-vis spectrum of $(\text{Fe}^{2+})\text{heme-HSA}$ is characterized by a broad Soret band centered at 418 nm, with a shoulder at 405 nm, and Q_1 and Q_0 bands at 536 and 572 nm, respectively (Figure 3, panel A, trace a). Moreover, the RR spectra (Figure 3, panel B, traces a and a'; Table 1) are in agreement with a previous magnetic circular dichroism (MCD) study,¹⁹ which showed that ferrous heme-HSA is a mixture of a 5cHS state, with Tyr161 coordinated to the heme iron, and a four-coordinate intermediate spin state (4cIS). It is noteworthy that an oxygen-bound pentacoordinate form is uncommon in ferrous heme proteins. The 413.1 nm excitation RR spectrum (Figure 3, panel B, trace a), in resonance with the Soret band, confirms the presence of two species, a 5cHS (ν_4 at 1358 cm^{-1} , ν_3 at 1472 cm^{-1} , ν_2 at 1557 cm^{-1} , ν_{10} at 1602 cm^{-1}) and a 4cIS (ν_4 at 1370 cm^{-1} , ν_3 at 1502 cm^{-1} , ν_2 at 1580 cm^{-1} , ν_{10} at 1635 cm^{-1}).³⁷ The 4cIS species is strongly enhanced in the RR spectrum obtained with 441.6 nm excitation (Figure 3, panel B, trace a'). In order to identify the nature of the fifth ligand in $(\text{Fe}^{2+})\text{heme-HSA}$ the spectra were also recorded upon addition of 2-MeIm, which is known to bind the heme giving rise to a 5cHS species.³⁸ Upon addition of 2-MeIm to $(\text{Fe}^{2+})\text{heme-HSA}$, the maximum of the Soret band red-shifts to 424 nm and, in the Q-band region, bands at 536, 559, 576 nm (Figure 3, panel A, trace b) were observed. The corresponding RR spectra, obtained with both 413.1 and 441.6 nm excitation (Figure 3, panel B, traces b and b'; Table 1), clearly indicate the presence of a 5cHS state (ν_4 at 1358 cm^{-1} , ν_3 at 1472 cm^{-1} , ν_{11} at 1555 cm^{-1} , ν_2 at 1562 cm^{-1} , ν_{10} at 1607 cm^{-1}) and a six-coordinate low spin (6cLS) species (ν_4 at 1358 cm^{-1} , ν_3 at 1493 cm^{-1} , ν_2 at 1582 cm^{-1} , ν_{10} at 1623 cm^{-1}). The corresponding spectra of the 2-MeIm- $(\text{Fe}^{2+})\text{heme}$ complex gave similar results (data not shown), which are also identical to those of the 2-MeIm- $(\text{Fe}^{2+})\text{heme}$ complex in cetyltrimethylammonium bromide (CTAB).^{39,40} $(\text{Fe}^{2+})\text{heme}$ in PBS at pH 6.9 is a mixture

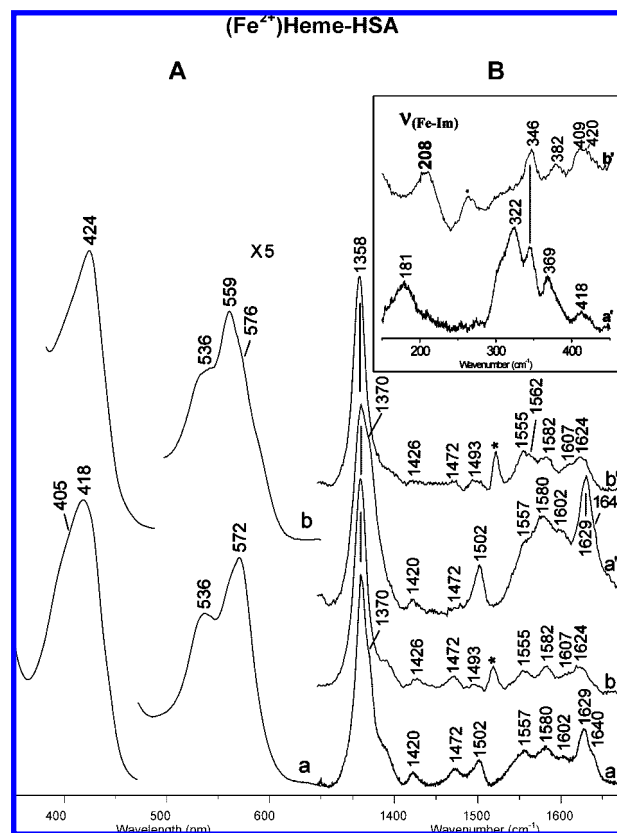


Figure 3. Panel A: absorption spectra of $(\text{Fe}^{2+})\text{heme-HSA}$ (a) and $(\text{Fe}^{2+})\text{heme-HSA}$ with 2-MeIm (b) in 0.08 M PBS at pH 6.9. Panel B: RR spectra of $(\text{Fe}^{2+})\text{heme-HSA}$ (a and a') and $(\text{Fe}^{2+})\text{heme-HSA}$ with 2-MeIm (b and b') in 0.08 M PBS at pH 6.9. Experimental conditions: (a) 413.1 nm excitation wavelength, 17 mW laser power at the sample, 1.1 cm^{-1} spectral resolution, 1800 s integration time; (a') 441.6 nm excitation wavelength, 25 mW laser power at the sample, 3.2 cm^{-1} spectral resolution, average of two spectra with 810 s integration time; (b) 413.1 nm excitation wavelength, 10 mW laser power at the sample, 3.8 cm^{-1} spectral resolution, average of two spectra with 304 s integration time; (b') 441.6 nm excitation wavelength, 20 mW laser power at the sample, 3.2 cm^{-1} spectral resolution, average of two spectra with 665 s integration time. The intensities are normalized to that of the ν_4 band at 1358 cm^{-1} . The inset of panel B shows the low frequency RR spectra of $(\text{Fe}^{2+})\text{heme-HSA}$, average of three spectra with 725 s integration time (a') and $(\text{Fe}^{2+})\text{heme-HSA}$ in the presence of 2-MeIm, 700 s integration time (b') at pH 6.9. The intensities are normalized to that of the 346 cm^{-1} band. The asterisk indicates a spurious band due to 2-MeIm.

of 5cHS and 4cIS species (data not shown) and becomes a mixture of 5cHS and 6cLS states upon addition of 2-MeIm.

In order to establish the nature of the fifth ligand for the $(\text{Fe}^{2+})\text{heme-HSA}$ in the presence and absence of 2-MeIm, RR spectra in the low frequency region were recorded. In fact, the low-frequency region RR spectra of His-bound five-coordinate ferrous hemoproteins are characterized by the presence of a strong band due to the iron-imidazole stretching mode, $\nu(\text{Fe-Im})$, which occurs in the region 200–250 cm^{-1} . Its frequency correlates with the bond strength between the iron atom and the imidazole ring.⁴¹ The inset in Figure 3 compares the RR spectra in the low-frequency region of heme-HSA in the absence (trace a) and presence of 2-MeIm (trace b). The

(34) Peisach, J.; Blumberg, W. E.; Ogawa, S.; Rachmilewitz, E. A.; Oltzik, R. *J. Biol. Chem.* **1971**, *246*, 3342–3355.

(35) Ghosh, K.; Thompson, A. M.; Goldbeck, R. A.; Shi, X.; Whitman, S.; Oh, E.; Zhiwu, Z.; Vulpe, C.; Holman, T. R. *Biochemistry* **2005**, *44*, 16729–16736.

(36) Tong, Y.; Guo, M. *J. Biol. Inorg. Chem.* **2007**, *12*, 735–750.

(37) Andersson, L. A.; Mylrajans, M.; Sullivan, E. P., Jr.; Strauss, S. H. *J. Biol. Chem.* **1989**, *264*, 19099–19102.

(38) Kincaid, J.; Stein, P.; Spiro, T. G. *Proc. Natl. Acad. Sci. U.S.A.* **1979**, *76*, 549–552.

(39) Ye, X.; Yu, A.; Georgiev, G. Y.; Gruia, F.; Ionascu, D.; Cao, W.; Sage, J. T.; Champion, P. M. *J. Am. Chem. Soc.* **2005**, *127*, 5854–5861.

(40) Gomez de Gracia, A.; Bordes, L.; Desbois, A. *J. Am. Chem. Soc.* **2005**, *127*, 17634–17643.

(41) Spiro T. G.; Li, X.-Y. *Resonance Raman Spectroscopy of Metalloporphyrins*. In *Biological Applications of Raman Spectroscopy*; Spiro, T. G., Ed.; Vol. 3; John Wiley & Sons: New York, 1988..

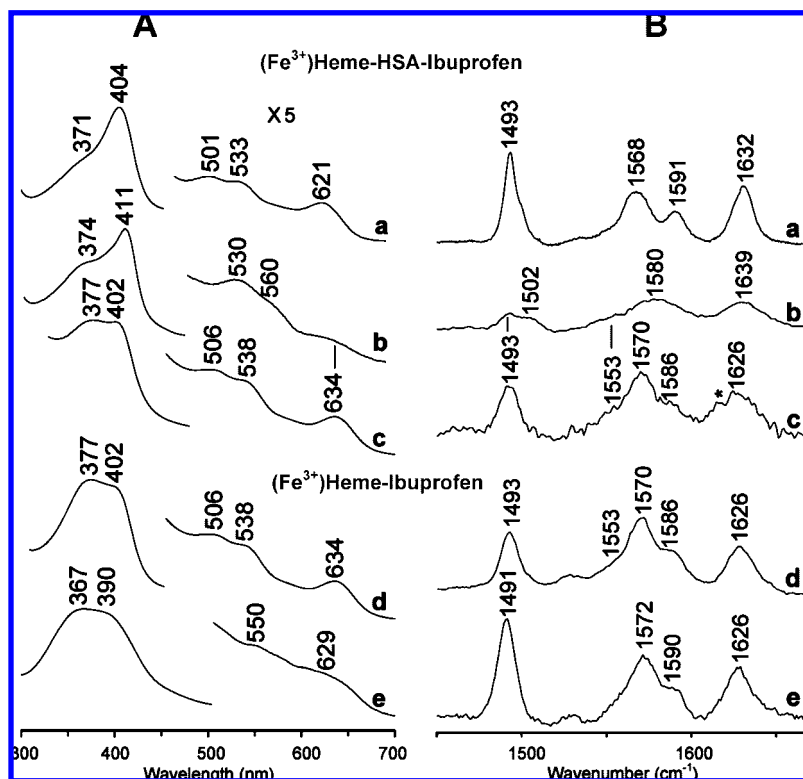


Figure 4. Absorption spectra (panel A) and RR spectra (panel B) of $(\text{Fe}^{3+})\text{heme}:\text{HSA}$ (molar ratio 1:4) (a), $(\text{Fe}^{3+})\text{heme-HSA-ibuprofen}$ (molar ratio 1:4:3000) (b), $(\text{Fe}^{3+})\text{heme-HSA-ibuprofen}$ (molar ratio 1:4:10000) (c), $(\text{Fe}^{3+})\text{heme-ibuprofen}$ (molar ratio 1:3000) (d), $(\text{Fe}^{3+})\text{heme}$ (e) in 0.08 M PBS at pH 6.9. Experimental conditions panel B: 406.7 nm excitation wavelength; (a) 15 mW laser power at the sample, 1 cm^{-1} spectral resolution, 3300 s integration time; (b) 3 mW laser power at the sample, 2.5 cm^{-1} spectral resolution, average of two spectra with 785 s integration time; (c) 3 mW laser power at the sample, 2.5 cm^{-1} spectral resolution, average of two spectra with 780 s integration time; (d) 4 mW laser power at the sample, 2.5 cm^{-1} spectral resolution, 1140 s integration time; (e) 25 mW laser power at the sample, 2.5 cm^{-1} spectral resolution, 900 s integration time. The intensities are normalized to that of the ν_4 band (not shown). The asterisk (panel B trace c) indicates a spurious band due to ibuprofen.

2-MeIm- $(\text{Fe}^{2+})\text{heme-HSA}$ adduct shows an intense band at 208 cm^{-1} , which corresponds to the 212 cm^{-1} band observed for the 2-MeIm adduct of heme in CTAB.³⁹ This band is due to the $\nu(\text{Fe-Im})$ stretching mode, and its lower frequency as compared to free heme indicates that the Fe-Im bond is weaker.

In conclusion, these results suggest that $(\text{Fe}^{2+})\text{heme-HSA}$ is a mixture of a Tyr-Fe 5cHS and a 4cIS species, as the weak Tyr ligand partially dissociates upon reduction. It is reasonable to expect that the two $(\text{Fe}^{3+})\text{heme-HSA}$ species, observed in the EPR spectra, give rise to two $(\text{Fe}^{2+})\text{heme-HSA}$ species. The species characterized by a weaker H-bonding transforms into the tetracoordinate IS form upon reduction, whereas the second $(\text{Fe}^{3+})\text{heme-HSA}$ species (stronger H-bonding) likely retains the Tyr coordination leading to the pentacoordinate ferrous form. Upon addition of 2-MeIm, the 4cIS and 5cHS ferrous states convert into the 5cHS and 6cLS states, respectively.

$(\text{Fe}^{3+})\text{Heme-HSA-Ibuprofen}$. Figure 4 shows the comparison of the UV-vis (panel A) and RR (panel B) spectra of the $(\text{Fe}^{3+})\text{heme-HSA}$ and of free $(\text{Fe}^{3+})\text{heme}$ in PBS in the absence and presence of increasing amounts of ibuprofen. No spectral changes in the UV-vis are apparent up to a $(\text{Fe}^{3+})\text{heme-HSA-ibuprofen}$ molar ratio of 1:4:500 (corresponding to 10 mM ibuprofen), where a broadening on the blue side of the Soret band and an intensity increase at about 560 nm are observed (data not shown). These changes become more evident upon addition of further amounts of the drug. The spectrum of $(\text{Fe}^{3+})\text{heme-HSA-ibuprofen}$ at a molar ratio 1:4:3000 (corresponding to 75 mM ibuprofen) (Figure 4, panel A, trace b) is markedly different from that of $(\text{Fe}^{3+})\text{heme-HSA}$

(Figure 4, panel A, trace a). The bands at 411, 530, 560 nm are typical of a 6cLS heme while the band at 374 nm, together with the weak band at about 634 nm, are due to a 5cHS species. Accordingly, the corresponding RR bands (Figure 4, panel B, trace b; Table 1) are assigned as follows: the bands at 1493 cm^{-1} to the ν_3 of the 5cHS form, and the bands at 1502, 1580, and 1639 cm^{-1} to the ν_3 , ν_2 , and ν_{10} , respectively, of a 6cLS species. CD spectra in the Soret region confirm the formation of a LS heme in the presence of ibuprofen, whereas only small changes are observed in the 200–280 nm region (data not shown).

At 75 mM ibuprofen concentration a change in the frequency of the propionyl bending mode is also observed, shifting from 373 (in the absence of the drug) to 378 cm^{-1} (in the presence of ibuprofen) (data not shown). A further increase of the ibuprofen concentration causes the disappearance of the LS species. The spectra become typical of a 5cHS form; the UV-vis spectrum (Figure 4, panel A, trace c) shows bands at 377 and 402 nm in the Soret region, at 506 and 538 nm in the Q-band region and a CT1 at 634 nm, while the RR spectrum (Figure 4, panel B, trace c) has core size marker bands at 1493 cm^{-1} (ν_3), 1553 cm^{-1} (ν_{11}), 1570 cm^{-1} (ν_2), 1586 cm^{-1} (ν_{37}) and 1626 cm^{-1} (ν_{10}). This HS form of $(\text{Fe}^{3+})\text{heme-HSA-ibuprofen}$ is different from that of $(\text{Fe}^{3+})\text{heme-HSA}$ (trace a). In fact, it is essentially identical to the spectrum obtained by mixing free heme with ibuprofen in the absence of HSA (trace d), but it is different from that of free heme in PBS (trace e). Hence, it corresponds to that of the heme dissociated from HSA and interacting with ibuprofen. The differences which can be

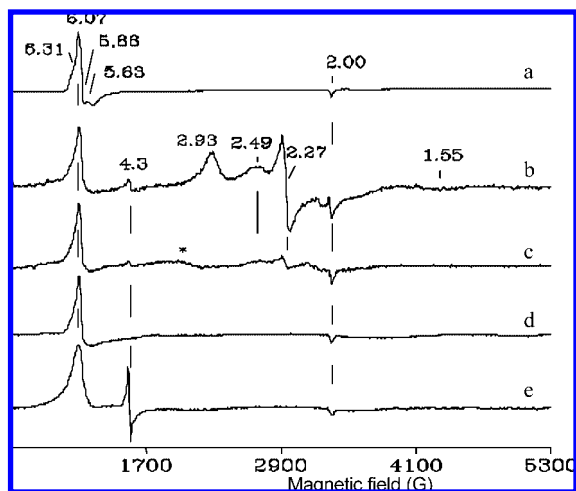


Figure 5. X-band EPR spectra of (Fe^{3+}) heme, (Fe^{3+}) heme-HSA and their complexes with ibuprofen at pH 6.9. The spectra were recorded at 5 K, 9.36 GHz microwave frequency, 1 mW microwave power, and 10 G modulation amplitude. (a) (Fe^{3+}) heme-HSA (molar ratio 1:4) in 0.1 M bicine; (b) (Fe^{3+}) heme-HSA-ibuprofen (molar ratio 1:4:3000) in 0.08 M PBS; (c) (Fe^{3+}) heme-HSA-IBU (molar ratio 1:4:10000) in 0.08 M PBS; (d) (Fe^{3+}) heme-ibuprofen (molar ratio 1:3000) in 0.08 M PBS; (e) (Fe^{3+}) heme in 0.1 M bicine. The asterisk (trace c) indicates a weak cavity signal. The feature at $g = 4.3$ results from a nonheme iron impurity.⁴⁰

noted in the Soret region between traces c and d are due to the excess ibuprofen present in sample c, which leads to the significant scattering in the absorption spectrum.

The EPR spectra have confirmed these results (Figure 5). Indeed, at the molar ratio of (Fe^{3+}) heme-HSA-ibuprofen (1:4:3000) which induces significant changes in the UV-vis and RR spectra, the corresponding EPR spectrum (trace b) is characterized by marked changes compared to the spectrum in the absence of ibuprofen (trace a). The spectrum of the ternary complex displays an axial HS species ($g_{\perp} = 6.07$) and two LS species ($g = 2.93, 2.27, 1.55$) and ($g = 2.49, 2.27$). The third g value of the latter species is not observed, likely due to its expected weak and broad character. The feature at $g = 4.3$ corresponds to a nonheme iron impurity often seen in biological samples.⁴² The axial HS signal with $g_{\perp} = 6.07$ has an identical line shape to that observed for the free heme sample with ibuprofen (Figure 5, trace d), whereas it is very different from that of free heme without ibuprofen (Figure 5, trace e) which is characterized by a much broader signal. In accord with the UV-vis and RR results, the analysis of EPR spectra suggests that the $g_{\perp} = 6.07$ signal corresponds to free heme dissociated from heme-HSA which interacts with the drug. Upon increasing the ibuprofen concentration, the EPR spectrum (Figure 5, trace c) is characterized essentially by the axial HS signal ($g_{\perp} = 6.07$) observed at lower ibuprofen concentrations, as the $g_1 = 2.93$ LS signal disappears and the $g_1 = 2.49$ LS signal is considerably reduced.

To gain insight into the possible axial ligands which give rise to the two LS species observed in the EPR spectra of (Fe^{3+}) heme-HSA-ibuprofen, the tetragonality (Δ/λ) and rhombicity (V/Δ) parameters have been determined from the g values.^{43,44} The values obtained for the $g = 2.93, 2.27, 1.55$ species ($\Delta/\lambda = 3.40, V/\Delta = 0.57$) place it in the H type group of the Blumberg and Peisach diagrams,⁴⁵ characterized by

systems having a bis-His axial coordination. However, such an assignment is not consistent with the crystal structure of HSA, which reveals the presence of only one His residue in the proximity of the heme binding site.¹³ In previous work, prior to the determination of the heme-HSA structure, the His residues which were considered able to bind the heme iron, were proposed to be His105^{46,47} and His242.⁴⁸ However, from the crystallographic structure of heme-HSA,¹³ it is clear that these residues are too distant from the heme. Only His146 is in the vicinity of the heme but at a distance of about 9 Å from the (Fe^{3+}) heme atom. If one accepts His146 as a probable axial ligand on one side of the heme, examination of the X-ray structure of (Fe^{3+}) heme-HSA without ibuprofen (Figure 1B)¹³ indicates the other axial ligand is the tyrosinate form of Tyr161 (although a water molecule cannot be completely excluded). In this reasonable scenario, we propose that the deviation of the crystal field parameters from those typical of His-Fe-OR systems^{45,49} may be the result of a strong hydrogen bond interaction, similar to the case reported previously for the His-Fe-O_{Tyr} center of a chloroplast hemoglobin.⁴⁹ Therefore, in the presence of ibuprofen the (Fe^{3+}) heme atom coordination of the 6cLS is proposed to be $\text{N}_{\text{His146}}-\text{Fe}-\text{O}_{\text{Tyr161}}$ in which the oxygen atom is strongly hydrogen bonded to one of the water molecules present in its proximity, as observed in the X-ray structure of (Fe^{3+}) heme-HSA without ibuprofen (Figure 1B).¹³ The heme coordination of the second LS species ($g = 2.49, 2.27$) is difficult to assign in the absence of the third g value. However, the two LS species should derive directly from the two HS species observed in the absence of ibuprofen. The LS species characterized by a H-bonded tyrosinate oxygen ($g = 2.93, 2.27, 1.55$) derives from the (Fe^{3+}) heme-HSA HS form in which the tyrosinate oxygen has a relatively strong H-bonding interaction. The axial coordination and H-bonding characteristics of the second LS species ($g = 2.49, 2.27$) are unclear, but it is perhaps reasonable to expect that it derives from the (Fe^{3+}) heme-HSA HS state with relatively weak H-bonding to the tyrosinate.

An attempt to identify the Fe-ligand by the assignment of the RR $\nu(\text{Fe}-\text{Im})$ stretching mode in (Fe^{2+}) heme-HSA-ibuprofen failed since this ternary complex is extremely unstable and the UV-vis and RR spectra changed both upon laser irradiation and with time.

CO- (Fe^{2+}) Heme-HSA Complexes. The protein matrix of the heme cavity has been probed by identification of the frequencies of the $\text{Fe}^{2+}-\text{CO}$ bands of the exogenous CO ligand complex. In fact, heme-bound CO is a sensitive probe for investigating distal and proximal effects on ligand binding of heme proteins since back-donation from the $\text{Fe } d_{\pi}$ to the CO π^* orbitals is modulated by polar interactions with protein residues, and by variations in the donor strength of the trans ligand.⁵⁰⁻⁵² As back-donation increases, the Fe-C bond strengthens while the CO bond weakens, thereby increasing the

(42) Hagen, W. R. *Dalton Trans.* **2006**, 4415-4434.

(43) Palmer, G. *Biochem. Soc. Trans.* **1985**, *13*, 548-560.

(44) Taylor, C. P. S. *Biochim. Biophys. Acta* **1977**, *491*, 137-149.

(45) Blumberg, W. E.; Peisach, J. In *Probes of Structure and Function of Macromolecules and Membranes*; Chance, B.; Yonetani, T.; Mildvan, A. S., Eds.; Academic Press: New York, 1971; pp 215-228.

(46) Dockal, M.; Chang, M.; Carter, D. C.; Rüker, F. *Protein Sci.* **2000**, *9*, 1455-1465.

(47) Fasano, M.; Baroni, S.; Vannini, A.; Ascenzi, P.; Aime, S. *J. Biol. Inorg. Chem.* **2001**, *6*, 650-658.

(48) Mattu, M.; Vannini, A.; Coletta, M.; Fasano, M.; Ascenzi, P. *J. Inorg. Biochem.* **2001**, *84*, 293-296.

(49) Das, T. K.; Couture, M.; Lee, H. C.; Peisach, J.; Rousseau, D. L.; Wittenberg, B. A.; Wittenberg, J. B.; Guertin, M. *Biochemistry* **1999**, *38*, 15360-15368.

(50) Spiro, T. G.; Wasbotten, I. H. *J. Inorg. Biochem.* **2005**, *99*, 34-44.

$\nu(\text{Fe}-\text{CO})$ vibrational frequencies and decreasing the $\nu(\text{CO})$ frequencies. For a large class of CO adducts of heme proteins and heme model compounds containing an imidazole as the fifth iron ligand, a linear correlation between the frequencies of the $\nu(\text{Fe}-\text{CO})$ and $\nu(\text{CO})$ stretching modes has been found. The correlation plots have a negative slope and depend on the extent of π -back-bonding. Furthermore, since Fe-CO back-bonding is also modulated by variations in the donor strength of the trans ligand, changes in the trans ligand donor strength shift the correlation line and give rise to parallel lines at higher or lower positions in the correlation plot.⁵⁰⁻⁵²

Upon addition of CO to $(\text{Fe}^{2+})\text{heme-HSA}$, the electronic absorption spectrum, similar to that previously reported,¹⁸ is characterized by a sharp Soret band centered at 416 nm and Q_1 and Q_0 bands at 536 and 559 nm, respectively (Figure 6, panel A, trace a). The spectrum differs from that of the free $(\text{Fe}^{2+})\text{heme}$ CO complex which is characterized by a Soret band at 411 nm.³⁹ Moreover, the blue-shift of the absorption bands compared to those of the CO complexes of heme proteins having an imidazole as fifth ligand, the Soret band normally appearing near 420 nm, suggests the presence of a $\text{CO}-(\text{Fe}^{2+})\text{heme}$ adduct with a trans ligand weaker than His,⁵¹ or no ligand at all.^{50,52}

Upon addition of ibuprofen to the $\text{CO}-(\text{Fe}^{2+})\text{heme-HSA}$ complex the UV-vis spectrum is characterized by bands at 421, 539, and 568 nm (Figure 6, panel A, trace c), similar to the spectrum of both the $\text{CO}-(\text{Fe}^{2+})\text{heme-HSA}$ complex in the presence of 2-MeIm (bands at 419, 539, and 567 nm; Figure 6, panel A, trace b) and of the $\text{CO}-(\text{Fe}^{2+})\text{heme-2-MeIm}$ complex.³⁹ This strongly suggests that a nitrogen atom is the trans-ligand of $\text{CO}-(\text{Fe}^{2+})\text{heme-HSA}$ in the presence of ibuprofen. Figure 6, panel B shows the RR spectra in the $\nu(\text{Fe}-\text{CO})$ and $\nu(\text{CO})$ stretching regions of $\text{CO}-(\text{Fe}^{2+})\text{heme-HSA}$. The isotopic shift observed by ¹³C substitution (data not shown) allowed us to identify the $\nu(\text{Fe}-\text{CO})$ and $\nu(\text{CO})$ stretching modes reported in Table 2.

In Figure 7 a plot of the $\nu(\text{Fe}-\text{CO})$ and $\nu(\text{CO})$ frequencies is reported for CO adducts of a variety of heme proteins and model compounds having either a histidine residue as the fifth ligand or a weaker/absent trans ligand. The lines are obtained according to eq 1 reported in ref 50. The slope represents the back-bonding sensitivity of $\nu(\text{FeC})$.

The frequencies of the stretching modes of some $\text{CO}-(\text{Fe}^{2+})\text{heme}$ complexes are shown in Table 2. The $\nu(\text{Fe}-\text{CO})$ stretching mode at 524 cm^{-1} and the $\nu(\text{CO})$ stretch at 1960 cm^{-1} of the $\text{CO}-(\text{Fe}^{2+})\text{heme-HSA}$ complex are located above the histidine line of the $\nu(\text{Fe}-\text{CO})/\nu(\text{CO})$ back-bonding correlation (Figure 7), indicating that the proximal ligand is either weak⁵² or absent,⁵¹ consistent with the presence of a trans Tyr ligand. In fact, inspection of Figure 7 reveals that the FeCO vibrational frequencies for $\text{CO}-(\text{Fe}^{2+})\text{heme-HSA}$ are located close to both those of $\text{CO}-(\text{Fe}^{2+})\text{heme}$ systems containing a weak trans oxygen ligand as in the case of (i) a water molecule, as for the His25Tyr mutant of human heme oxygenase-1 (hHO-1),⁵³ (ii) a Tyr ligand, such as in the hemophore HasA from *Serratia marcescens* (HasA_{SM})²⁸ and to CO-heme complexes with no trans ligand, as in the case of

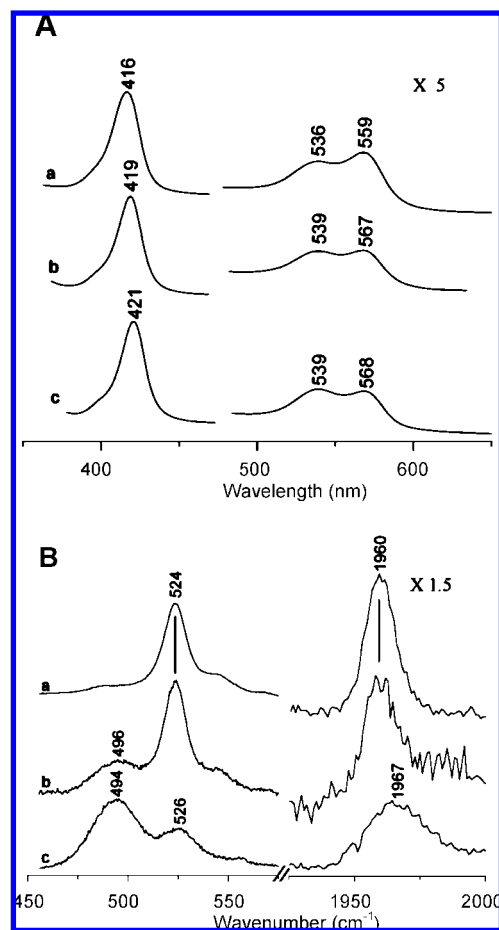


Figure 6. Absorption spectra (panel A) and RR spectra (panel B) of $\text{CO}-(\text{Fe}^{2+})\text{heme-HSA}$ (molar ratio 1:4) (a), $\text{CO}-(\text{Fe}^{2+})\text{heme-HSA-2MeIm}$ (molar ratio 1:4:15000) (b), $\text{CO}-(\text{Fe}^{2+})\text{heme-HSA-ibuprofen}$ (molar ratio 1:4:3000) (c) in 0.08 M PBS at pH 6.9. Experimental conditions panel B: 413.1 nm excitation wavelength; 1 cm^{-1} and 3.3 cm^{-1} spectral resolution for the low and high frequency region, respectively; (a) 15 mW laser power at the sample; average of 32 spectra with 140 s integration time (low frequency region); average of three spectra with 600 s integration time (high frequency region); (b) 2 mW laser power at the sample; integration time 2400 s (low frequency region); average of three spectra with 1800 s integration time (high frequency region); (c) 3 mW laser power at the sample, integration time 2100 s (low frequency region); average of six spectra with 1800 s integration time (high frequency region). The intensities are normalized to that of the ν_4 band (not shown).

the $(\text{Fe}^{2+})\text{heme-CO}$ adduct in glycerol.³⁹ However, the correlation plot cannot effectively separate a 5c CO system from a 6c species with a weak proximal ligand, such as water or Tyr.^{39,50}

Upon addition of 2-MeIm, together with the bands at 524 and 1960 cm^{-1} due to the $\text{CO}-(\text{Fe}^{2+})\text{heme-HSA}$ complex, a new weak $\nu(\text{Fe}-\text{CO})$ band at 496 cm^{-1} is observed. Because of the weakness of this form we are unable to distinguish the corresponding $\nu(\text{CO})$ band which, in analogy with $\text{CO}-(\text{Fe}^{2+})\text{heme}$ model compounds having 2-MeIm as the trans ligand, is expected to be around 1960 cm^{-1} .^{50,54} Therefore, this band should overlap with the $\nu(\text{CO})$ mode of the $\text{CO}-(\text{Fe}^{2+})\text{heme-HSA}$ form. A change of the excitation wavelength from 413.1 to 406.7 nm leads to a substantial enhancement of the 524 cm^{-1} band relative to the 496 cm^{-1} band (data not shown),

(51) Vogel, K. M.; Kozłowski, P. M.; Zgierski, M. Z.; Spiro, T. G. *Inorg. Chim. Acta* **2000**, *297*, 11–17.

(52) Ray, G. B.; Li, X. Y.; Ibers, J. A.; Sessler, J. L.; Spiro, T. G. *J. Am. Chem. Soc.* **1994**, *116*, 162–176.

(53) Liu, Y.; Moëne-Loccoz, P.; Hildebrand, D. P.; Wilks, A.; Loehr, T. M.; Mauk, A. G.; Ortiz de Montellano, P. R. *Biochemistry* **1999**, *38*, 3733–3743.

(54) Kalodimos, C. G.; Gerotheranassis, I. P.; Hawkes, G. E. *Biospectroscopy* **1998**, *4*, S57–S69.

Table 2. Vibrational Frequencies (cm^{-1}) of the FeCO Stretching Modes in CO Adducts of Selected Iron Porphyrins and Heme Proteins^a

protein ^b	$\nu(\text{FeCO})$	$\nu(\text{CO})$	axial ligation	reference
6c CO Complexes with Weak Trans Ligand or 5c Complexes with No Ligand				
1. heme-HSA + ibuprofen	525 (519)	1962 (1924)	CO-Fe	this work
2. heme-HSA + 2-MeIm	524 (520)	1960 (1912)	CO-Fe-O _{Tyr}	this work
3. heme-HSA	524 (520)	1960 (1912)	CO-Fe-O _{Tyr}	this work
4. HasA _{SM}	532 (523)	1954 (1905)	CO-Fe-O _{Tyr}	28
5. human HO-1(H25Y)	529 (524)	1962 (1917)	CO-Fe-H ₂ O	53
6. heme-CO (80% glycerol)	530 (525)	1955	CO-Fe-?	39
7. heme-CO in PBS, pH 6.9	525	1962	CO-Fe	this work
6c CO Complexes with Imidazole Trans Ligand and Apolar Distal Environment				
8. heme-HSA + ibuprofen	494 (488)	1967 (1924)	CO-Fe-N _{His}	this work
9. heme-HSA + 2-MeIm	496 (492)	1960 (1912)	CO-Fe-N _{His}	this work
10. Fe(PPDME)(Im)	495	1960	CO-Fe-N _{His}	61
11. HRP, pH 3	492	1967	CO-Fe-N _{His}	55
12. sperm whale Mb, pH 2.6	491	1967	CO-Fe-N _{His}	56, 57
13. H64G Mb, pH 7	492	1965	CO-Fe-N _{His}	58
14. H64A Mb, pH 7	490	1966	CO-Fe-N _{His}	59, 60
15. H64V Mb, pH 7	488	1967	CO-Fe-N _{His}	59, 60
16. H64I Mb, pH 7	490	1968	CO-Fe-N _{His}	59, 60
17. H64L Mb, pH 7	490	1965	CO-Fe-N _{His}	59, 60

^a The frequencies obtained with ¹³CO are given in parentheses. ^b HasA_{SM}, hemophore HasA from *Serratia marcescens*; HO-1, heme oxygenase-1; HRP, horseradish peroxidase; Mb, myoglobin; PPDME, protoporphyrin IX dimethyl ester.

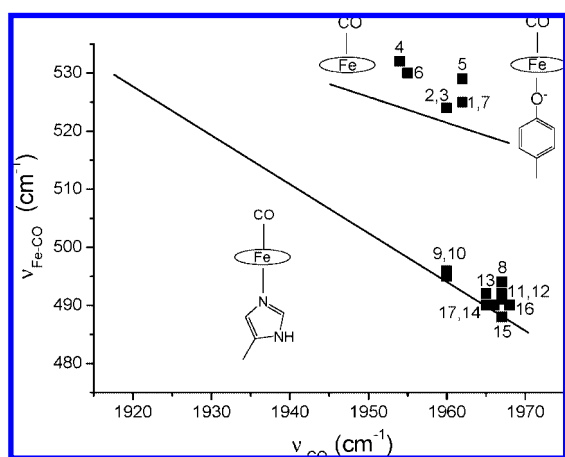


Figure 7. Plot of the $\nu(\text{FeCO})$ versus $\nu(\text{CO})$ frequencies observed in the CO complexes of heme-HSA under various experimental conditions, together with representative heme proteins and model compounds taken as references. The numbers correspond to the entries in Table 2. The lower line indicates the back-bonding correlation line for six-coordinate CO heme proteins with imidazole as sixth ligand, as given in ref 50. The upper line represents five-coordinate, with no trans ligand, or six-coordinate CO heme proteins with weak trans ligands. The inset figures show the respective trans ligands.

suggesting that the two forms derive from two Soret bands which overlap, giving a resultant maximum at 419 nm.

In the presence of ibuprofen, two CO-(Fe²⁺)heme-HSA forms (characterized by $\nu(\text{Fe-CO})$ and $\nu(\text{CO})$ frequencies at 525, 1962 cm^{-1} and at 494, 1967 cm^{-1} , respectively) are observed upon 413.1 nm excitation. The relative intensity of these forms depends on the excitation wavelength, and the former species is enhanced for 406.7 nm excitation and almost completely absent with 441.6 nm excitation (Figure S2 of Supporting Information). Therefore, the less abundant form corresponds to a free heme-CO species bound to the drug which is characterized by $\nu(\text{Fe-CO})$ at 525 cm^{-1} and $\nu(\text{CO})$ at 1962 cm^{-1} (data not shown). The most abundant species, with $\nu(\text{Fe-CO})$ at 494 cm^{-1} and $\nu(\text{CO})$ at 1967 cm^{-1} , falls on the histidine $\nu(\text{Fe-CO})/\nu(\text{CO})$ back-bonding correlation line (Figure 7) in the region which is typical of the heme complexes where CO is surrounded by a weakly polar environment. In fact, it is

clear from Figure 7 that this form falls very close to that of horseradish peroxidase (HRP) at acidic pH,⁵⁵ myoglobin (Mb) at acidic pH,^{56,57} Mb mutants where the distal His(67) is replaced by apolar residues,⁵⁸⁻⁶⁰ and the model compound imidazole-protoporphyrin IX dimethyl ester [(Fe(PPDME)(Im))].⁶¹ This confirms that upon binding of ibuprofen to heme-HSA a major conformational change occurs in the heme pocket allowing the imidazole ring of a His residue to bind the heme Fe atom via its N atom. The formation of the Fe-N bond is convincingly confirmed by the presence of the $\nu(\text{Fe-Im})$ stretching mode upon photolysis of the CO in the laser beam. Figure 8 shows the low frequency region RR spectra obtained with 441.6 nm excitation of the CO-(Fe²⁺)heme-HSA complex in the presence of ibuprofen upon increasing the laser power. At 1 mW laser power (Figure 8, trace a), when CO is fully bound (ν_4 at 1372 cm^{-1}) the $\nu(\text{Fe-CO})$ at 494 cm^{-1} is fairly strong. At higher laser power (8 and 35 mW, Figure 8 traces b and c, respectively), CO is partially photolyzed. Therefore, the CO mode decreases in intensity and the vibrations of the ferrous 5c species grow in (ν_4 at 1355 cm^{-1}). The strong band which appears at 218 cm^{-1} is therefore assigned to the $\nu(\text{Fe-Im})$ mode and demonstrates the coordination of an imidazole ring to (Fe²⁺)heme-HSA upon ibuprofen binding.

Discussion

In analogy with other previous spectroscopic measurements,^{18,19} the RR, UV-vis, and EPR spectroscopic characterization reported herein indicates that in solution the ferric heme binds to HSA, giving rise to a 5cHS species containing Tyr161 as

- (55) Smulevich, G.; Paoli, M.; De Sanctis, G.; Mantini, A. R.; Ascoli, F.; Coletta, M. *Biochemistry* **1997**, *36*, 640-649.
 (56) Ramsden, J.; Spiro, T. G. *Biochemistry* **1989**, *28*, 3125-3128.
 (57) Sage, J. T.; Morikis, D.; Champion, P. M. *Biochemistry* **1991**, *30*, 1228-1237.
 (58) Morikis, D.; Champion, P. M.; Springer, B. A.; Sligar, S. G. *Biochemistry* **1989**, *28*, 4791-4800.
 (59) Li, T. S.; Quillin, M. L.; Phillips, G. N.; Olson, J. S. *Biochemistry* **1994**, *33*, 1433-1446.
 (60) Ling, J. H.; Li, T. S.; Olson, J. S.; Bocian, D. F. *Biochim. Biophys. Acta* **1994**, *1188*, 417-421.
 (61) Evangelista-Kirkup, R.; Smulevich, G.; Spiro, T. G. *Biochemistry* **1986**, *25*, 4420-4425.

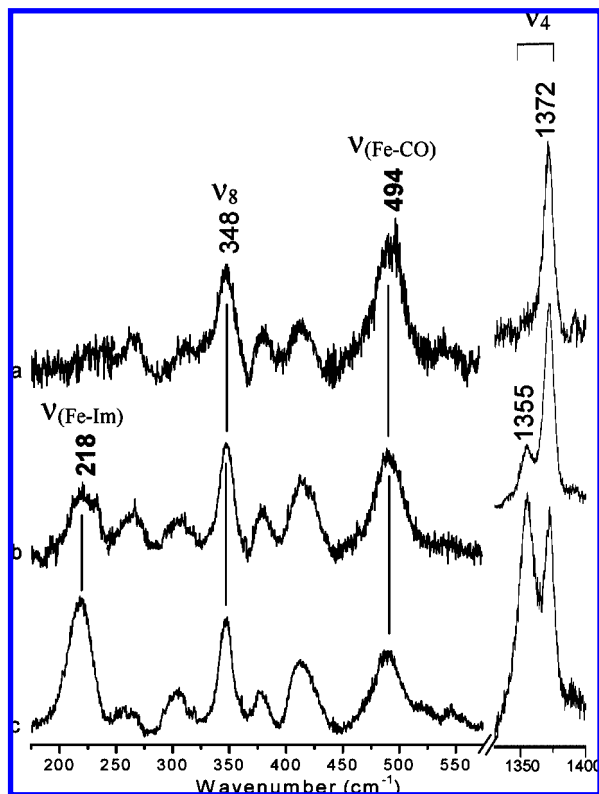


Figure 8. RR spectra of CO-(Fe²⁺)heme-HSA-ibuprofen (molar ratio 1:4:3000) in 0.08 M PBS at pH 6.9. Experimental conditions: 441.6 nm excitation wavelength, 0.9 cm⁻¹ spectral resolution, (a) 1 mW laser power at the sample, average of eight spectra with 1800 s integration time (low frequency region), average of five spectra with 1800 s integration time (high frequency region); (b) 8 mW laser power at the sample, average of six spectra with 750 s integration time (low frequency region), average of three spectra with 1800 s integration time (high frequency region); (c) 35 mW laser power at the sample, average of two spectra with 900 s integration time (low frequency region), 132 s integration time (high frequency region). The intensities are normalized to that of the ν_4 band.

the axial ligand. In agreement with the long Fe-O_{Tyr} bond (2.73 Å) observed in the crystal structure,¹³ the oxygen atom is weakly bound and upon reduction is partially detached resulting in a mixture of a 5c and 4c species. The considerable spectral variations induced by ibuprofen binding to (Fe³⁺)heme-HSA indicate a change of heme spin state from 5cHS to 6cLS. Furthermore, as the amount of the drug increases, the affinity¹⁶ of the heme for HSA decreases, leading to heme dissociation. Hence, it is apparent that ibuprofen binding to (Fe³⁺)heme-HSA causes an allosteric conformational transition.

Ibuprofen binds to HSA at Sudlow's site 2 ($K_d = 3.7 \times 10^{-7}$ M)^{8,62} and to a secondary binding cleft (with $K_d = 4 \times 10^{-5}$ M)¹⁶ that has been located on domain II at the interface between subdomains IIA and IIB.³ The affinity of ibuprofen for HSA decreases by 1 order of magnitude for the heme-HSA complex.¹⁶ The reciprocal influence of heme and drug binding on their respective affinities for HSA clearly indicates that their binding sites are linked. Interestingly, because of its flexible three-domain structure, HSA can be considered as a prototype of monomeric proteins displaying allosteric properties. In particular, both homotropic and

heterotropic interactions are known to modulate the conformational transition(s) between two or more conformational states, depending on ligand binding. Considering fatty acids as a physiological HSA ligand, binding of fatty acids determines a spatial rearrangement of the three domains that indeed affects binding of fatty acids to other sites (homotropic interactions). Conversely, binding of drugs to fatty acid sites may affect the affinity of fatty acids to different clefts and vice versa. Accordingly, on the basis of Wyman's theory,⁶³ drug binding sites, the heme binding site, and fatty acid binding sites may be considered functionally linked through a rearrangement(s) of domain II with respect to domains I and III,^{1,2,16,17,64-67} as observed in oligomeric proteins (e.g. hemoglobin).

Structural and solution studies of ibuprofen binding to HSA have shown that the ibuprofen primary binding site does not appear to be functionally linked to the heme primary site, whereas the secondary site is located within domain II at the interface between domains IIA and IIB.^{3,64} This site is in close functional and structural contact with the Sudlow's site 1, i.e., the warfarin binding site, which is linked to the heme binding site.^{3,64,68} Accordingly, as noted previously,⁶⁴ occupancy of the ibuprofen secondary site is expected to affect the heme binding site. Thus, it appears likely that ibuprofen binding to the secondary binding site triggers the allosteric conformational transition which has the considerable structural consequences on the heme binding pocket observed spectroscopically in this study. Therefore, the conformational adaptability of HSA involves more than the immediate vicinity of the drug binding sites.

A comprehensive analysis of the experimental data from each of the techniques applied to the present study (UV-vis, RR, and EPR) suggests that in both the ferric and ferrous states of heme-HSA, the 6cLS species observed in the presence of ibuprofen has a His residue bound to the heme Fe atom. In fact, the level of confidence in this unexpected result, which requires considerable disruption of the heme cavity, is enhanced by its repeated finding using complementary techniques. Furthermore, these results are in agreement with the observation that warfarin and ibuprofen binding to NO-(Fe²⁺)heme-HSA induces a transition from a pentacoordinate to hexacoordinate state, characterized by a His residue coordinated to the heme Fe atom.¹⁶ On the basis of the crystal structure of (Fe³⁺)heme-HSA,¹³ the only His residue able to bind the heme iron atom is His146. This residue is at a distance of about 9 Å from the heme Fe atom; therefore, significant changes in the heme cavity site are envisioned. The heme is located within the subdomain IB, which is constituted by the subdomain-connecting loop and the four contiguous helices 7, 8, 9, and 10. The distal and proximal sides of the heme pocket are enclosed by helices 8 and 9, which contain His146 and Tyr161, respectively¹³ (Figure 1, panel B). The secondary binding site of ibuprofen

(63) Wyman, J. *Adv. Protein Chem.* **1964**, *19*, 223-286.

(64) Fanali, G.; Bocedi, A.; Ascenzi, P.; Fasano, M. *FEBS J.* **2007**, *274*, 4491-4502.

(65) Bocedi, A.; Notari, S.; Menegatti, E.; Fanali, G.; Fasano, M.; Ascenzi, P. *FEBS J.* **2005**, *272*, 6287-6296.

(66) Chuang, V. T.; Otagiri, M. *Pharm. Res.* **2002**, *19*, 1458-1464.

(67) Fitos, I.; Visy, J.; Kardos, J. *Chirality* **2002**, *14*, 442-448.

(68) Fanali, G.; Ascenzi, P.; Fasano, M. *Biophys. Chem.* **2007**, *129*, 29-35.

(62) Whitlam, J. B.; Crooks, M. J.; Brown, K. F.; Pedersen, P. V. *Biochem. Pharmacol.* **1979**, *28*, 675-678.

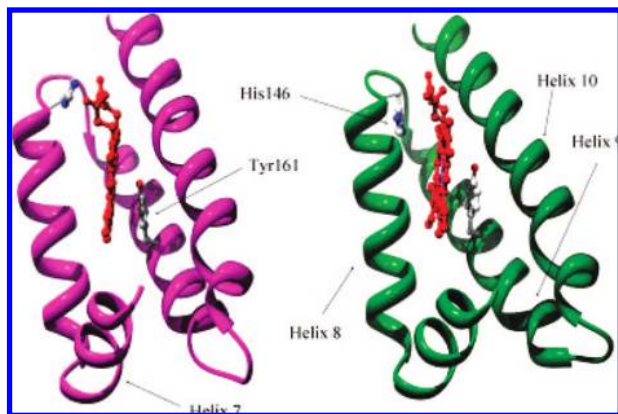


Figure 9. Mechanism proposed to explain the formation of the $\text{O}_{\text{Tyr}}\text{-Fe-N}_{\text{His146}}$ 6cLS species in the heme–HSA–ibuprofen complex. Purple ribbon: the heme binding domain in the heme–HSA complex (PDB entry 1O9X¹⁴). Green ribbon: model obtained by energy minimization of the heme (red) structure within the heme binding cleft of the HSA–ibuprofen complex (PDB entry 2BXG³). Residues potentially involved in heme Fe^{3+} coordination (i.e., His146 and Tyr161) are indicated. For further details, see text.

is located at the IIA–IIB interface establishing contacts with domain IIIA (Figure 1, panel A), allowing more protein flexibility.

An attempt is made in Figure 9 to establish the possible structural consequences on the heme binding site which result from occupancy of the ibuprofen secondary site. In Figure 9 the purple ribbon shows the heme–HSA structure (1O9X¹⁴) whereas the green ribbon represents the heme binding domain obtained by energy minimization of the heme (red) structure within the heme binding cleft of the HSA–ibuprofen complex (2BXG³). Comparison of these two structures shows that occupancy of the ibuprofen secondary site may lead to a distortion of the heme binding site with an appreciable tilt of helix 10 and a reorientation of helix 7. Hence, we may hypothesize that the formation of the $\text{N}_{\text{His146}}\text{-Fe-O}_{\text{Tyr161}}$ 6cLS species upon ibuprofen binding derives from a shift of helix 8 (as a consequence of the reorientation of helix 7) that leads to a rotation of the His146 residue toward the heme Fe^{3+} atom. In the model, His146 is distant 7.2 Å from the Fe atom, but clearly further rearrangements can be expected following heme entry into its site. The extent of the rearrangements to the heme cavity following ibuprofen binding is underscored by the observed frequency change of the RR propionyl bending mode from 373 to 378 cm^{-1} in the presence of ibuprofen. This indicates a modification of the interactions of the heme propionic residues, which in the absence of ibuprofen protrude from the pocket, forming two important salt bridges with His146 and with Lys190.¹³ In fact, the frequency of this band has been correlated with the hydrogen bond strength between the heme-propionate and the nearby amino acid residues. The band shifts to higher frequency as the hydrogen bonding increases through addition of more bonds or an increase in the bond strength of existing bonds.^{69,70} Moreover, the slight changes also observed in the frequency of the $\nu(\text{C}=\text{C})$ vinyl stretches upon addition of ibuprofen to the (Fe^{3+}) heme–HSA complex are consistent

with a readjustment of the heme binding site induced by ibuprofen binding (see Supporting Information). Interestingly, comparison of the HSA structures (containing myristate) in the presence and absence of heme reveals that three residues, namely Arg114, His146, and Lys190 show pronounced movements upon heme complexation.¹³ His146 displays perhaps the largest movement upon complexation, making a key salt bridge with the ‘A’ ring carboxylate of the heme, resulting in an equidistant His N_{ϵ} atom to O1A/O2A distance of 3.30 Å. Moreover, ibuprofen binding to HSA³ causes a marked change of the Arg186 position, which is part of the heme binding pocket.¹³ Therefore, it is perhaps not unexpected that drug binding to (Fe^{3+}) heme–HSA can cause a repositioning of the His146 residue.

Conclusions

The spectroscopic characterization of (Fe^{3+}) heme–HSA is consistent with a 5cHS heme containing a weak $\text{Fe}^{3+}\text{-O}_{\text{Tyr}}$ coordination, in agreement with the fairly long $\text{Fe}^{3+}\text{-O}$ distance (2.73 Å) determined from the crystal structure. The weak Tyr ligand partially dissociates upon reduction. Moreover, the pentacoordinate tyrosine-bound heme coordination of heme–HSA, observed in the absence of ibuprofen, becomes hexacoordinate low spin upon ibuprofen binding. The electronic absorption spectrum and $\nu(\text{Fe-CO})/\nu(\text{CO})$ vibrational frequencies of the heme–HSA–ibuprofen CO complex together with the observation of a Fe–His Raman mode at 218 cm^{-1} upon photolysis of the CO complex and the low spin EPR g values indicate that a His residue is one of the low spin axial ligands, the sixth ligand probably being Tyr161.

We suggest that the His146 residue, distant 9 Å in the absence of the drug, binds the heme iron as a consequence of a significant rearrangement of the heme pocket following the drug binding to heme–HSA. These results imply that the conformational adaptability of HSA involves more than the immediate vicinity of the drug binding site. As a consequence of the functional link of the heme pocket to the ibuprofen secondary site, heme and drug (e.g., ibuprofen) plasma levels are reciprocally influenced, with the possibility of unexpected variations in the effective concentration of therapeutic agents bound to the ibuprofen secondary site following hemolytic events. In parallel, heme scavenging by HSA appears to be modulated by ibuprofen and drug binding to the ibuprofen secondary site.

The therapeutic efficiency of drugs present in the plasma can be seriously compromised by their high binding affinity for HSA. This represents a significant drawback in the pharmacological treatment of diseases, as to achieve 90% drug action a concentration of at least 1 order of magnitude higher appears to be required in the presence of plasma proteins than in their absence. Conversely, the increase of plasmatic levels of ferric heme under pathological conditions may induce a massive release of drugs with the concomitant intoxication of the patient. Moreover, the free heme plasma level could increase in patients under drug therapy; this is dangerous for tissues and organs since the heme–iron catalyzes the formation of reactive oxygen species.^{1,2,17,64,71,65}

As a whole, the present spectroscopic investigation supports the notion that HSA could be considered as the

(69) Gottfried, D. S.; Peterson, E. S.; Sheikh, A. G.; Wang, J.; Friedman, J. M. *J. Phys. Chem.* **1996**, *100*, 12034–12042.

(70) Cerda-Colón, J. F.; Silfa, E.; López-Garriga, J. *J. Am. Chem. Soc.* **1998**, *120*, 9312–9317.

(71) Bocedi, A.; Notari, S.; Narciso, P.; Bolli, A.; Fasano, M.; Ascenzi, P. *IUBMB Life* **2004**, *56*, 609–614.

prototype of monomeric allosteric proteins. Given the fundamental importance of HSA in determining pharmacokinetic properties of several drugs, and in turn their biological efficacy by modulating drug availability, allosteric regulation of drug binding to HSA is particularly important in pharmacological therapy management.

Acknowledgment. This work was funded by grants from the Università di Firenze (ex 60%) (to G.S.), the Ministero dell'Istruzione, dell'Università e della Ricerca (MIUR), Italy (to M. Fittipaldi), and the Università dell'Insubria (FAR) (to M. Fasano). The authors express their gratitude to Dr. A. Feis

(Università di Firenze) for several fruitful discussions and to Profs. M. Coletta (Università La Sapienza, Roma) and G. De Sanctis (Università di Camerino) for the CD measurements.

Supporting Information Available: RR vinyl mode analysis and the excitation wavelength dependence of the RR spectra of CO-(Fe²⁺)heme-HSA-ibuprofen. This material is available free of charge via the Internet at <http://pubs.acs.org>.

JA800966T